Purinergic Signalling (2016) 12:313–329
DOI 10.1007/s11302-016-9506-7

ORIGINAL ARTICLE

Role of extracellular cysteine residues in the adenosine A_{2A} receptor

Elisabetta De Filippo[1] · Vigneshwaran Namasivayam[1] · Lukas Zappe[1] · Ali El-Tayeb[1] · Anke C. Schiedel[1] · Christa E. Müller[1]

Received: 4 January 2016 / Accepted: 29 February 2016 / Published online: 11 March 2016

Abstract The G protein-coupled A_{2A} adenosine receptor represents an important drug target. Crystal structures and modeling studies indicated that three disulfide bonds are formed between ECL1 and ECL2 (I, Cys71$^{2.69}$-Cys159$^{45.43}$; II, Cys74$^{3.22}$-Cys146$^{45.30}$, and III, Cys77$^{3.25}$-Cys166$^{45.50}$). However, the A_{2B}AR subtype appears to require only disulfide bond III for proper function. In this study, each of the three disulfide bonds in the A_{2A}AR was disrupted by mutation of one of the cysteine residues to serine. The mutant receptors were stably expressed in Chinese hamster ovary cells and analyzed in cyclic adenosine monophosphate (cAMP) accumulation and radioligand binding studies using structurally diverse agonists: adenosine, NECA, CGS21680, and PSB-15826. Results were rationalized by molecular modeling. The observed effects were dependent on the investigated agonist. Loss of disulfide bond I led to a widening of the orthosteric binding pocket resulting in a strong reduction in the potency of adenosine, but not of NECA or 2-substituted nucleosides. Disruption of disulfide bond II led to a significant reduction in the agonists' efficacy indicating its importance for receptor activation. Disulfide bond III disruption reduced potency and affinity of the small adenosine agonists and NECA, but not of the larger 2-substituted agonists. While all the three disulfide bonds were essential for high potency or efficacy of adenosine, structural modification of the nucleoside could rescue affinity or efficacy at the mutant receptors. At present, it cannot be excluded that formation of the extracellular disulfide bonds in the A_{2A}AR is dynamic. This might add another level of G protein-coupled receptor (GPCR) modulation, in particular for the cysteine-rich A_{2A} and A_{2B}ARs.

Keywords A_{2A} adenosine receptor · A_{2B} adenosine receptor · Cysteine · Disulfide bonds · GPCR · Mutagenesis

Introduction

Adenosine receptors (ARs) belong to the class of purinergic G protein-coupled receptors (GPCRs); they are divided into four subtypes: A_1, A_{2A}, A_{2B}, and A_3. These receptors are widely expressed in the body and are involved in a number of physiological and pathological processes [1, 2]. The four ARs are potential drug targets for the treatment of neurodegenerative [3], immune [4], cardiac [5], and inflammatory disorders [6, 7] and cancer [8]. Recently, pharmaceutical companies have been investing in the development of A_{2A}AR antagonists as a monotherapy or in combination with antibodies targeting inhibitory check points, e.g., programmed cell death 1 protein (PD-1) or its ligand PD-L1, pursuing an immunochemotherapeutic approach [9]. The purine nucleoside adenosine (**1**, Fig. 1) physiologically activates ARs showing different affinities for each subtype [10]. The signaling pathway involves G_i protein coupling for A_1 and A_3 AR subtypes, leading to an inhibition of adenylate cyclase and a reduction in cyclic adenosine monophosphate (cAMP) production. In contrast, A_{2A} and A_{2B} ARs preferentially couple to G_s proteins thereby increasing intracellular cAMP accumulation [1]. Among the four AR subtypes, A_{2A} and A_{2B} AR are the closest homologs displaying a sequence identity of 58 % and a

Electronic supplementary material The online version of this article (doi:10.1007/s11302-016-9506-7) contains supplementary material, which is available to authorized users.

✉ Christa E. Müller
christa.mueller@uni-bonn.de

[1] Pharma Center Bonn, Pharmaceutical Institute, Pharmaceutical Chemistry I, University of Bonn, An der Immenburg 4, 53121 Bonn, Germany

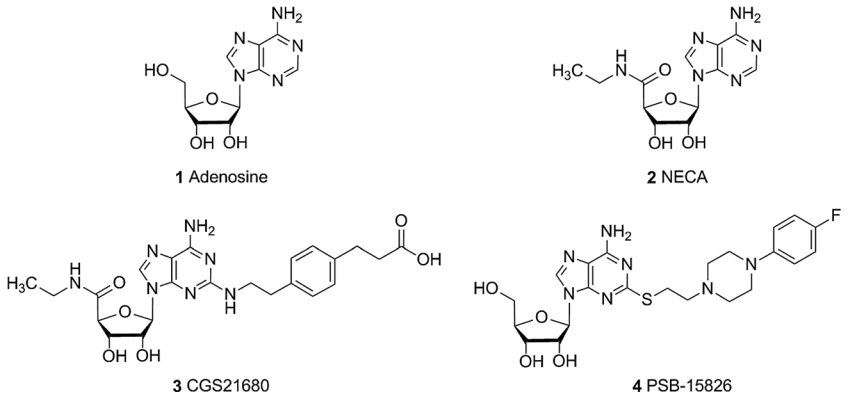

Fig. 1 Chemical structures of investigated adenosine receptor agonists

similarity of 73 %. Sequence analysis of the human A_{2A} and A_{2B} ARs revealed the largest differences in the loop regions, especially in the extracellular loop 2 (ECL2) [11]. The endogenous ligand adenosine and its derivatives NECA (**2**) and CGS21680 (**3**) show significantly higher affinity for the A_{2A}AR than for the A_{2B} receptor subtype, despite very similar ligand binding sites of both receptors [12, 13]. The structural reason for this striking difference is unknown.

The extracellular loops of GPCRs may be involved in ligand binding and receptor activation [14]. In class A GPCRs, including ARs, the ECL2 is the largest and most diverse of the three ECLs. Its high variety even within subfamilies has been associated with ligand selectivity [15–19]. Most class A GPCRs contain disulfide bonds in their extracellular domains rigidifying the receptor structure. Several mutagenesis studies and X-ray structures [20–23] showed that the ECL2 adopts different conformations during the activation mechanism, switching between an open and a closed state. In a previous study by de Graaf et al., the ECL2 sequences of 365 human non-olfactory GPCRs were aligned, and the number of cysteine residues was analyzed [24]. The A_{2A} and A_{2B} AR subtypes were found to have the highest number of cysteine residues in the ECL2 among the investigated GPCRs, namely three (A_{2A}), or four (A_{2B}) (Fig. 2). In most rhodopsin-like GPCRs, two highly conserved cysteine residues are present near the extracellular surface forming a disulfide bond which has been shown to be essential for receptor structure and activation [27, 28]. Both, A_{2A} and A_{2B} AR subtypes, possess two of the cysteine residues that were found to be highly conserved in most class A GPCRs: $Cys^{45.50}$ in the ECL2 and $Cys^{3.25}$ located at the extracellular end of transmembrane domain 3 (TMD3) (Ballesteros Weinstein nomenclature [29] and ECL nomenclature proposed by de Graaf et al. [24]). Despite the high sequence similarity between A_{2A} and A_{2B}ARs, discrepant data are available regarding the structure of the extracellular region of the two AR subtypes. Crystal structures of the A_{2A}AR as well as a subsequent molecular modeling study indicated that four disulfide bonds were formed in that receptor (Fig. 2): three linking the ECL2 with the ECL1 ($Cys71^{2.69}$-$Cys159^{45.43}$ (I), $Cys74^{3.22}$-$Cys146^{45.30}$ (II), and $Cys77^{3.25}$-$Cys166^{45.50}$ (III), Fig. 2), and the fourth one forming an intra-loop bond in the ECL3 ($Cys259^{6.61}$-$Cys262^{6.64}$) [25, 30–33].

Similarly, it was shown by mutagenesis studies that in the closely related A_{2B}AR, the two cysteine residues conserved in class A GPCRs ($Cys78^{3.25}$ in TM3 and $Cys171^{45.50}$ in ECL2, corresponding to disulfide bond III of the A_{2A}AR (Fig. 2)), form a disulfide bond, which plays an essential role in ligand binding and receptor activation [11]. On the contrary, mutations of the other three cysteine residues present in the ECL2 of the A_{2B}AR (Cys154, Cys166, and Cys167) only slightly affected receptor activation indicating that the potential disulfide bonds formed by those cysteine residues are not critical for A_{2B}AR function [11]. In addition, another purinergic receptor, $P2Y_{12}$, which is activated by ADP, was found by X-ray crystallography to form the "GPCR-conserved" disulfide bond found in almost all class A GPCRs only in the presence of the agonists 2MeSADP and 2MeSATP [20, 34] but not when the non-nucleotidic competitive antagonist AZD1283 was bound to the receptor [20]. Further mutagenesis studies showed that the conserved cysteine residues were not essential for the binding of the antagonist AZD1283 suggesting the possibility of a dynamic disulfide bond in $P2Y_{12}$ receptors [20].

For these reasons, an investigation appears necessary to explain the contradictory results regarding the number of essential extracellular cysteine residues and disulfide bonds in the two closely related AR subtypes A_{2A} and A_{2B}. Recently, a mutagenesis study on the A_{2A}AR was published in which extracellular cysteine residues of the A_{2A}AR were mutated to alanine [35]. The authors suggested that the formation of the "GPCR-conserved" disulfide bond $Cys77^{3.25}$-$Cys166^{45.50}$ was neither essential for receptor localization at the cell surface nor for ligand binding [35]. Their investigation was purely based on radioligand binding utilizing a single, 2-substituted adenosine derivative, CGS21680 in each cysteine mutant; functional data of the cysteine mutant receptors were not provided. In the present study, we present a comprehensive investigation on the importance of extracellular disulfide bonds in the A_{2A}AR. We generated three A_{2A}AR mutants

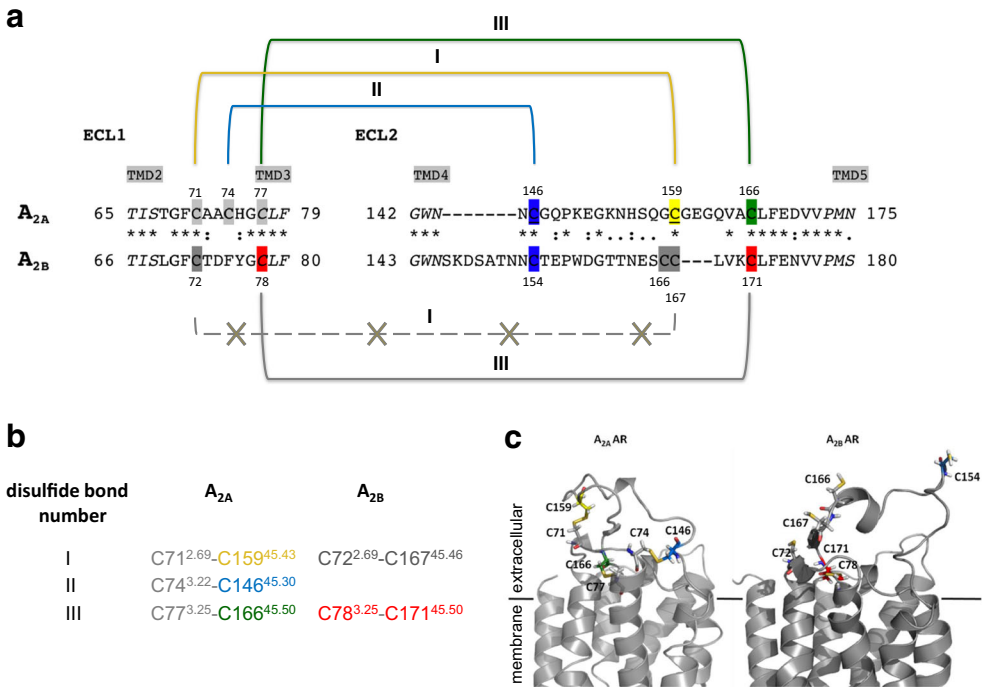

Fig. 2 Cysteine residues and disulfide bonds in the extracellular loop 1 and 2 of the human A_{2A} and A_{2B} ARs. The amino acid sequence alignment (**a**) of ECL1 and 2 of A_{2A} and A_{2B} ARs was done using ClustalW [11]. The following cysteine residues in the ECL2 of the A_{2A}AR are highlighted according to the colors of the cysteine mutants: *blue* $C146^{A2A}$, *yellow* $C159^{A2A}$, *green* $C166^{A2A}$. The other extracellular cysteine residues in the A_{2A}AR are highlighted in *light gray*. In the A_{2B}AR, the essential cysteine residues found by a mutagenesis study [11] are indicated in *red*. The identical amino acid residues (*), the conserved amino acid substitutions (:), and the semi-conserved amino acid substitutions (.) in both receptor subtypes are indicated. The positions of the cysteine residues are given for the A_{2A} and A_{2B} ARs. **b** The disulfide bonds found in the crystal structure of A_{2A}AR [25] and the corresponding ones in the A_{2B}AR are designated *I*, *II*, and *III*. **c** 3D homology models of A_{2A}AR based on the CGS21680-bound crystal structure 4UHR and of A_{2B}AR based on the A_{2A}AR X-ray structure 3EML [25, 26]. Cysteine residues are represented as *sticks* and color-coded according to (**a**)

replacing each cysteine residue present in the ECL2 ($Cys146^{45.30}$, $Cys159^{45.43}$, and $Cys166^{45.50}$) by the sterically and electronically similar amino acid serine, thereby disrupting one of the potential disulfide bonds in each mutant receptor. In addition, considering the high homology to the closely related A_{2B}AR subtype, we created an A_{2A}AR double mutant exchanging the two cysteine residues in the ECL2 ($Cys146^{45.30}$ and $Cys159^{45.43}$) which were supposed to be involved in disulfide bonds with the ECL1, thereby disrupting two potential disulfide bonds in a single mutant receptor. The goal of the current study was to investigate the importance of extracellular disulfide bonds in the A_{2A}AR for ligand binding and receptor activation by various agonists including the endogenous ligand adenosine.

Material and methods

Materials

Cell culture media, supplements, and antibiotics were obtained from Invitrogen (Darmstadt, Germany). Chemicals were purchased from Sigma-Aldrich (Taufkirchen, Germany), Roth (Karlsruhe, Germany), or Applichem (Darmstadt, Germany), unless otherwise noted. [^{3}H]cAMP (specific activity 34 Ci/mmol) and [^{3}H]NECA (17 Ci/mmol) were obtained from Amersham-GE Healthcare (Frankfurt, Germany) while [^{3}H]CGS21680 (36.05 Ci/mmol) was from Perkin Elmer (Rodgau, Germany). All enzymes and competent bacteria were purchased from New England Biolabs (Frankfurt, Germany). Primers and pcDNA3.1(−) vector were obtained from Invitrogen (Darmstadt, Germany), while the retroviral vector pQCXIN was purchased from Clontech (Heidelberg, Germany). Adenosine deaminase (ADA) was purchased from Sigma-Aldrich (Taufkirchen, Germany), Ro20-1724 (4-(3-butoxy-4-methoxyphenyl)methyl-2-imidazolidone) from Hoffmann La Roche (Grenzach, Germany), and the scintillation cocktail LUMASAFE from Perkin Elmer (Rodgau, Germany). Adenosine and NECA were obtained from Sigma-Aldrich (Taufkirchen, Germany), BAY60-6583 (2-[[6-amino-3,5-dicyano-4-[4-(cyclopropylmethoxy)phenyl]-2-pyridinyl]thio]acetamide) and CGS21680 (2-*p*-(2-carboxyethyl)phenethylamino-5′-*N*-ethylcarboxamidoadenosine) from Tocris (Wiesbaden-Nordenstadt, Germany), and PSB-15826 (2-(4-(4-fluorophenyl)piperazin-1-yl)ethylthioadenosine) was

synthesized at the Pharmaceutical Institute of the University of Bonn (El-Tayeb A., Müller C. E. et al. unpublished).

Site-directed mutagenesis

The coding sequence of the human A_{2A}AR was cloned into the pcDNA3.1(−) vector, and point mutations corresponding to single amino acid mutations were inserted with site-directed mutagenesis using the polymerase chain reaction (PCR). Oligonucleotide primers included the corresponding mismatch flanked by 14–15 nucleotides at the 3′- and 5′- end. The PCR reaction mixture consisted of 20 ng of template DNA, 15 pmol of each forward and reverse primer, 10 mM dNTPs, 1 × Q5 buffer, and 1 U of Q5 High Fidelity Polymerase (New England Biolabs, Frankfurt, Germany). The PCR was carried out as follows: 4 min at 94 °C, 20 cycles consisting of 1 min at 94 °C, 1 min at 66 °C and 10 min at 72 °C followed by a final elongation step of 10 min at 72 °C. The obtained DNA was digested by a methylation-sensitive restriction enzyme, DpnI, and then transformed into *Escherichia coli* Top10. Single clones were isolated, and the plasmid DNA was sequenced by GATC Biotech (Konstanz, Germany). Mutated receptors were finally subcloned into the retroviral vector pQCXIN.

Cell culture

Chinese hamster ovary (CHO) cells were cultured at 37 °C with 5 % CO_2 in Dulbecco's modified eagle medium-F12 (DMEM-F12) containing 10 % fetal calf serum (FCS), 100 U/ml penicillin G, and 100 μg/ml streptomycin. GP + envAM12 packaging cells [36] were cultured at 37 °C, 5 % CO_2 in hypoxanthine/xanthine/mycophenolic acid (HXM) medium which consists of DMEM, 10 % FCS, 100 U/ml penicillin G, 100 μg/ml streptomycin, 1 % ultraglutamine, 0.2 mg/ml hygromycin B, 15 μg/ml hypoxanthine, 250 μg/ml xanthine, and 25 μg/ml mycophenolic acid.

Retroviral transfection

CHO cells stably expressing the human A_{2A}AR, the human A_{2B}AR and the mutant A_{2A} receptors, were generated with a retroviral transfection system. GP + envAM12 packaging cells were seeded in DMEM medium containing 10 % FCS, 100 U/ml penicillin G, and 100 μg/ml streptomycin into a flask 24 h before the transfection. The cells were then transfected with the receptor DNA (6.75 μg) and the vesicular stomatitis virus G protein DNA (VSV-G, 3.75 μg) using Lipofectamine 2000 (Invitrogen, Karlsruhe, Germany). After 15 h of incubation, the medium was removed and replaced by 3 ml of DMEM medium containing 10 % FCS, 100 U/ml penicillin G, and 100 μg/ml streptomycin, including 5 mM sodium butyrate. The packaging cells were incubated at 32 °C with 5 % CO_2 for 48 h. Then the supernatant of the GP + envAM12 cells was filtered, mixed with 6 μl of polybrene solution (4 mg/ml), and incubated with CHO cells for 2.5 h at 37 °C. After 48 h, the cells were selected using 0.8 mg/ml of geneticin, G418. After two weeks, the concentration of G418 was reduced to 0.2 mg/ml.

Cell surface expression

The cell surface expression of the human A_{2A}AR, the human A_{2B}AR and the cysteine mutant receptors in CHO cells, was verified by enzyme-linked immunosorbent assay (ELISA); 200,000 cells/well were seeded into 24-well plates 24 h before the assay. Cells were washed with phosphate-buffered saline (PBS), blocked for 5 min with 1 % bovine serum albumin (BSA)/PBS, and then incubated with an human influenza hemagglutinin (HA) antibody solution (Covance, Munich, Germany), diluted 1:1000 in 1 % BSA/PBS, for 1 h at room temperature (rt). After washing with PBS, cells were fixed with a cold 1:1 (*v*/*v*) methanol/acetone solution for 15 min at −20 °C, washed and blocked again under the same conditions as described above. The horseradish peroxidase-coupled secondary antibody (goat anti-mouse, Sigma, Munich, Germany) was diluted 1:5000 in 1 % BSA/PBS and incubated for 1 h with the cells at rt. Finally, the cells were washed with PBS and incubated for 50 min with 300 μl of ABTS (2,2′-azino-bis(3-ethylbenzothiazoline-6-sulfonic acid)) substrate (Thermo Scientific Pierce, Rockford, USA). An aliquot of the substrate (170 μl) was transferred into a 96-well plate, and the absorbance was measured at 405 nm. Independent experiments were performed in triplicates.

Determination of cAMP accumulation

CHO cells (200,000 cells/well) were seeded into 24-well plates 24 h before performing the assay. Cells were then washed and incubated for 2 h at 37 °C and 5 % CO_2 in Hank's balanced salt solution (HBSS; 20 mM HEPES (4-(2-hydroxyethyl)-1-piperazineethanesulfonic acid), 13 mM NaCl, 5.5 mM glucose, 5.4 mM KCl, 4.2 mM $NaHCO_3$, 1.25 mM $CaCl_2$, 1 mM $MgCl_2$, 0.8 mM $MgSO_4$, 0.44 mM KH_2PO_4, and 0.34 mM Na_2HPO_4, pH 7.4) with 1 U/ml of ADA. Where adenosine was tested as an agonist, ADA was omitted. Cells were then incubated 15 min with the phosphodiesterase inhibitor Ro20-1724 (final concentration 40 μM) at 37 °C and 5 % CO_2. Different dilutions of agonist in 5 % DMSO (dimethylsulfoxide)/HBSS buffer (final DMSO concentration: 1 %) were added to the cells and incubated for 15 min under the same conditions described above. The supernatant was then removed, and 500 μl of hot lysis buffer (90 °C; 4 mM EDTA (ethylenediaminetetraacetic acid) and 0.01 % Triton X-100, pH 7.4) was added. After one hour of mixing on ice, the cAMP (cyclic adenosine monophosphate)

amount in the lysates was determined by competitive radioligand binding [4]. An aliquot of lysate (50 μl) was incubated with 30 μl of [^{3}H]cAMP solution in lysis buffer (final radioligand concentration 3 nM) and 40 μl of cAMP-binding protein (50 μg/vial) [37]. For the cAMP standard curve, 50 μl of different cAMP concentrations were measured instead of cell lysate. Total binding was obtained by mixing radioligand solution and cAMP-binding protein with lysis buffer, and the background was defined in the absence of binding protein. For experiments under reducing conditions, cells were preincubated for 2 h with a final concentration of 10 mM dithiothreitol (DTT). The mixture was incubated for 60 min on ice and then filtered through GF/B glass fiber filters using a Brandel harvester. The filters were then washed with ice-cold Tris buffer (2-amino-2-(hydroxymethyl)propane-1,3-diol; 50 mM, pH 7.4), transferred into vials, and incubated for 6 h with 2.5 ml of scintillation cocktail LUMASAFE. The vials were then counted in a liquid scintillation counter (Tricarb 2900TR, Perkin Elmer, Rodgau, Germany). Independent experiments were performed in duplicates. Amounts of cAMP were calculated by linear regression from a standard curve and normalized to the maximal effect induced by 100 μM of forskolin (set equal to 100 %).

Membrane preparation

Stably transfected CHO cells were cultured in dishes until confluency. In order to increase the exogenous protein expression, valproic acid was added (final concentration: 0.5 mg/ml) one day before harvesting [38]. Then cells were washed with sterile PBS and scraped off using ice-cold Tris buffer (5 mM Tris and 2 mM EDTA, pH 7.4). The cell suspension was homogenized and centrifuged for 10 min at 1000*g* to remove unbroken cells and nuclei. The supernatant was centrifuged at 30000*g* for 60 min. The pellet was resuspended in ice-cold 50 mM Tris-HCl buffer (pH 7.4) and stored at −80 °C until used. Protein concentrations were determined by the Bradford method [39].

Radioligand binding

Competition experiments were performed with [^{3}H]CGS21680 and [^{3}H]NECA in a final volume of 400 μl. The vial contained 10 μl of dissolved test compound in DMSO, 90 μl of Tris buffer (50 mM, pH 7.4), 100 μl of $MgCl_2$ solution (final concentration: 10 mM), 100 μl of radioligand solution (final radioligand concentration: [^{3}H]CGS21680, 5 nM; [^{3}H]NECA, 3 nM), and 100 μl of membrane preparation (70–150 μg/vial), which was previously incubated with 2 U of adenosine deaminase per milligram of protein for 20 min. Total binding was measured in the absence of test compound, while non-specific binding was determined in the presence of 50 μM NECA in experiments with [^{3}H]CGS21680, and 100 μM of N^6-(*R*)-(2-phenylisopropyl)adenosine (*R*-PIA) in experiments with [^{3}H]NECA. After incubation ([^{3}H]CGS21680, 1 h; [^{3}H]NECA, 3 h), the assay mixture was filtered through GF/B glass fiber filters using a Brandel harvester (Brandel, Gaithersburg, USA). The filters were washed three times with 300 μl ice-cold Tris buffer (50 mM, pH 7.4), transferred into scintillation vials and incubated for 6 h with 2.5 ml of scintillation cocktail LUMASAFE. The vials were then counted in a liquid scintillation counter (Tricarb 2900TR, Perkin Elmer, Rodgau, Germany). Independent experiments were performed in duplicates. In the homologous competitive binding, a single concentration of radiolabeled ligand and various concentrations of the identical unlabeled ligand were used. For the analysis, it is assumed that the system is at equilibrium and that both hot and cold ligands bind with identical affinities. Thus, the K_D and K_i values are identical. With the Cheng and Prussoff equation, the K_i value is calculated from the IC_{50} resulting in $K_d = K_i = IC_{50}$—[radioligand].

Molecular docking

The recent co-crystal structure of the human A_{2A}AR with the agonist CGS21680 (4UHR.pdb) was obtained from the RCSB (Research Collaboratory for Structural Bioinformatics) Protein Data Bank [32]. The agonist structure PSB-15826 was docked into the binding pocket of the A_{2A}AR using AutoDock 4.2 [40]. As an initial step, the co-crystallized water molecules and the ligand were removed from the X-ray structure. The hydrogen atoms were added and protonated using Protonate in Molecular Operating Environment (MOE 2014.08) [41]. The AutoDockTools package was applied to calculate the partial charges, generate the docking input files, and analyze the docking results [40]. Three-dimensional energy scoring grids of 60 × 60 × 60 points with a spacing of 0.375 Å were computed. To define the binding pocket for the docking procedure, the grids were centered based on the co-crystallized ligand. In the final step, PSB-15826 was docked into the binding site using the search algorithm Lamarckian Genetic Algorithm and the default scoring function, which is a hybrid scoring function (semi-empirical and free-energy) implemented in AutoDock4.2. The putative binding mode of PSB-15826 was selected on the basis of the lowest binding energy and visual inspection of the interactions. For obtaining a comparison with the binding conformation of NECA and adenosine, the respective X-ray crystal structures (PDB ID 2YDO and 2YDV) were downloaded from the RCSB protein data bank and superimposed on the structure obtained with CGS21680 [31]. For the mutant receptors, we generated a receptor model by substituting the residues using the protein builder and minimization modules of MOE2014.08.

Results

Potential role of disulfide bonds in the adenosine A_{2A} receptor

The relevance of disulfide bond formation for the function of the A_{2A}AR was experimentally observed by treating A_{2A}-expressing CHO cells with a reducing agent, dithiothreitol (DTT), followed by agonist-induced cAMP accumulation assays. As shown in Fig. 3, reducing of the disulfide bonds accessible to DTT caused a rightward shift of the dose-response curves obtained by NECA or by CGS21680 stimulation, respectively, in comparison with untreated cells. NECA-induced cAMP production was more affected than CGS21680-induced cAMP accumulation. After DTT treatment, the potency of NECA at the A_{2A}AR was 100-fold lower (EC_{50} values: 6.81 ± 1.27 vs. 606 ± 12 nM) while the potency of CGS21680 was only reduced by 6-fold (EC_{50} values: 22.6 ± 3.6 vs. 119 ± 6 nM). The DTT treatment did not cause any non-specific effect on cAMP accumulation levels at A_{2A}AR-expressing CHO cells, neither on the baseline (after DTT treatment: 3.22 ± 0.72 cpm and without DTT treatment: 5.23 ± 1.29 cpm; $n = 6$, two-tailed t test: not significantly different) nor on the forskolin-stimulated cAMP level (after DTT treatment: 94.4 ± 15.2 cpm and without DTT treatment: 101 ± 8 cpm, $n = 6$, two-tailed t test: not significantly different).

Generation and characterization of mutant cell lines

Since the initial DTT experiments suggested that disulfide bonds play an important role in A_{2A}AR function, the next step was to generate A_{2A} mutant receptors by site-directed mutagenesis, exchanging a single cysteine residue present in the ECL2 (C146, C159, or C166) for a serine residue. This led to the disruption of a single disulfide bond between ECL1 and ECL2 in each of the cysteine mutants (C146S, C159S, and C166S), see Fig. 2. A fourth A_{2A} receptor mutant was generated by replacing both cysteine residues, that are not conserved in class A GPCRs, in the ECL2 (C146S-C159S) thereby disrupting two disulfide bonds at the same time.

After the CHO cell lines that stably expressed the cysteine A_{2A} mutant receptors had been established, their cell surface expression was compared to that of the wild type (wt) A_{2A}AR by enzyme-linked immunosorbent assay (ELISA; see Table 1). For this purpose, each receptor had been linked at the N terminus to a human influenza hemagglutinin (HA) tag, which was previously shown not to interfere with receptor function or ligand binding [11, 42]. In addition, cysteine mutant receptors were analyzed by homologous competition binding using CGS21680 versus the agonist radioligand [^{3}H]CGS21680 and calculating B_{max} and K_D values (Table 1). Differently, from the ELISA which was performed with intact cells to detect only receptor surface expression, this method was performed with cell membranes thereby quantifying the density of receptors present in all membranes, including intracellular ones. Moreover, the agonist radioligand [^{3}H]CGS21680 may preferably label the active receptor conformation although binding has been shown to be not nucleotide-sensitive [43].

The mutant C159S A_{2A} receptor showed a significant gain in affinity (3-fold) for CGS21680 and a higher cell surface expression level (227 %) than the wt A_{2A}AR (100 %). Both, the single mutant C166S and the double mutant C146S-C159S receptors, displayed somewhat lower expression levels than the wt A_{2A}AR as determined by ELISA (40 and 87 % of the wt expression, respectively) and homologous binding experiments (48 and 74 % of the wt expression, respectively). A different radioligand, [^{3}H]NECA (3 nM), was used to

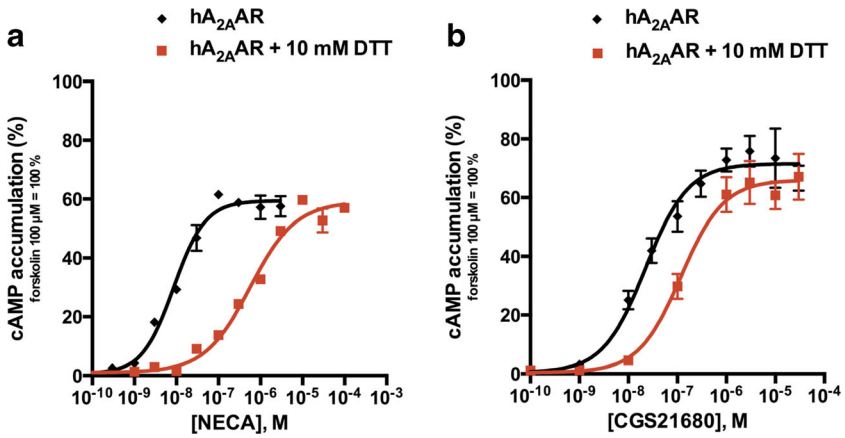

Fig. 3 Effect of DTT on activation of the human A_{2A}AR. cAMP accumulation induced by NECA (**a**) and CGS21680 (**b**) in CHO cells stably expressing the human A_{2A}AR with and without DTT pretreatment (10 mM, 2 h, 37 °C). Data represent means ± SEM of two independent experiments performed in duplicates. Determined EC_{50} values for NECA: without DTT: 6.81 ± 1.27 nM; after DTT pretreatment: 606 ± 12 nM***. EC_{50} values for CGS21680: without DTT: 22.6 ± 3.6 nM; after DTT pretreatment: 119 ± 6 nM**. (Two-tailed t test: $^{**}p < 0.01$ and $^{***}p < 0.001$)

Table 1 Expression levels (B_{max}) and K_D values of the wt human A_{2A} receptor and the A_{2A} cysteine mutants. Data are obtained by homologous binding versus [^{3}H]CGS21680 (5 nM; upper table) and [^{3}H]NECA (3 nM; lower table). Data are means ± SEM of the three independent experiments, unless otherwise noted. ELISA data are shown for comparison between the wt $hA_{2A}AR$ and the mutants

[^{3}H]CGS21680	K_D ± SEM (nM)	B_{max} ± SEM (fmol/mg of protein)	ELISA (%)
hA_{2A} wt	127 ± 3	478 ± 70	100 ± 16
hA_{2A} C166S	110 ± 4[b, ns]	230 ± 38[a, **]	40.1 ± 12.4[***]
hA_{2A} C159S	46.2 ± 6.5[a, ***]	421 ± 51[ns]	227 ± 4[***]
hA_{2A} C146S – C159S	124 ± 10[b, ns]	352 ± 78[b, ns]	87.4 ± 15.2[*]
[^{3}H]NECA			
hA_{2A} wt	6.33 ± 1.42	129 ± 13	100 ± 16
hA_{2A} C146S	25.8 ± 5.9[*]	152 ± 17 [ns]	23.0 ± 6.5[***]

[n.d] not determined, because of the low expression of the hA_{2A} C146S mutant; [ns] not significantly different from wt $hA_{2A}AR$ (determined using the two-tailed *t* test)

[a] $n = 4$

[b] $n = 5$

[*] $p < 0.05$

[**] $p < 0.01$

[***] $p < 0.001$

determine K_D and B_{max} values of the C146S mutant, because of the narrow window between total and non-specific binding values obtained with the less affine radioligand [^{3}H]CGS21680. While the cell surface expression of the C146S mutant receptor was found to be significantly decreased in comparison to the wt $A_{2A}AR$ (23 % of the wt expression determined by ELISA), the B_{max} value determined in membrane preparations was not significantly different from that of the wt receptor.

Receptor activation

The function of the A_{2A} receptor mutants was investigated by agonist-induced cAMP accumulation assays (Fig. 4) and compared to that of the wt $A_{2A}AR$ as well as the homologous $A_{2B}AR$. Structurally diverse agonists were tested: the endogenous agonist adenosine (**1**, Fig. 1), its close analog NECA (**2**), the 2-substituted acidic agonist CGS21680 (**3**), and the 2-substituted uncharged adenosine derivative PSB-15826 (**4**). The response of the endogenous agonist adenosine at all cysteine mutant receptors was significantly altered in comparison with the wt $A_{2A}AR$ (EC_{50} values and efficacies are listed in Table 2). At three cysteine mutants adenosine displayed significantly reduced potency (22-fold at C159S, 30-fold at C166S, and 253-fold at C146S-C159S) whereas at the C146S mutant, adenosine induced almost no activation (maximal effects: 4 ± 1 vs. 44 ± 3 % of forskolin activation). Upon analyzing the receptors' activation by other agonists, we noticed that the C166S mutant receptor showed only minor potency changes for the adenosine derivatives NECA, CGS21680, and PSB-15826 compared to the wt $A_{2A}AR$ (Table 2). The C146S mutant receptor could be moderately activated by NECA and CGS21680 (efficacies: 20 and 18 % vs. 55 and 52 %, respectively) while it showed no activation by PSB-15826. A gain in potency was found at the C159S mutant receptor for all the adenosine derivatives (10-fold for NECA, 6-fold for CGS21680, and 21-fold for PSB-15826). The activity of the double mutant C146S-C159S was more affected by smaller agonists (potency loss: 253-fold for adenosine and 87-fold for NECA) than the larger ones (EC_{50} values similar to wt $A_{2A}AR$ for CGS21680 and PSB-15826, Table 2).

Radioligand binding studies

Competitive binding experiments versus the radioligand [^{3}H]CGS21680 (Fig. 5) were used to determine the affinity of the cysteine A_{2A} mutant receptors for the selected agonists (K_i values are listed in Table 3). Adenosine was not tested in binding experiments since cell membrane preparations already contain endogenous adenosine and are normally pretreated with adenosine deaminase to remove endogenous adenosine. A biphasic behavior was observed for NECA binding at the C159S mutant receptor, with a low K_i value of 4.92 nM that was 16-fold lower in comparison to the wt $A_{2A}AR$ (81.2 nM). The C166S mutant receptor characterized by a disruption of the "GPCR-conserved" disulfide bond showed similar affinity for the adenosine derivatives NECA and CGS21680 as the wt $A_{2A}AR$, and a slight but significant reduction in affinity (1.7-fold) for PSB-15826 (see Table 3). The double mutant receptor C146S-C159S significantly lost affinity (30-fold) for the small ligand NECA while only a slight decrease (2-fold) was observed for PSB-15826 in comparison with the wt $A_{2A}AR$. The agonist radioligand

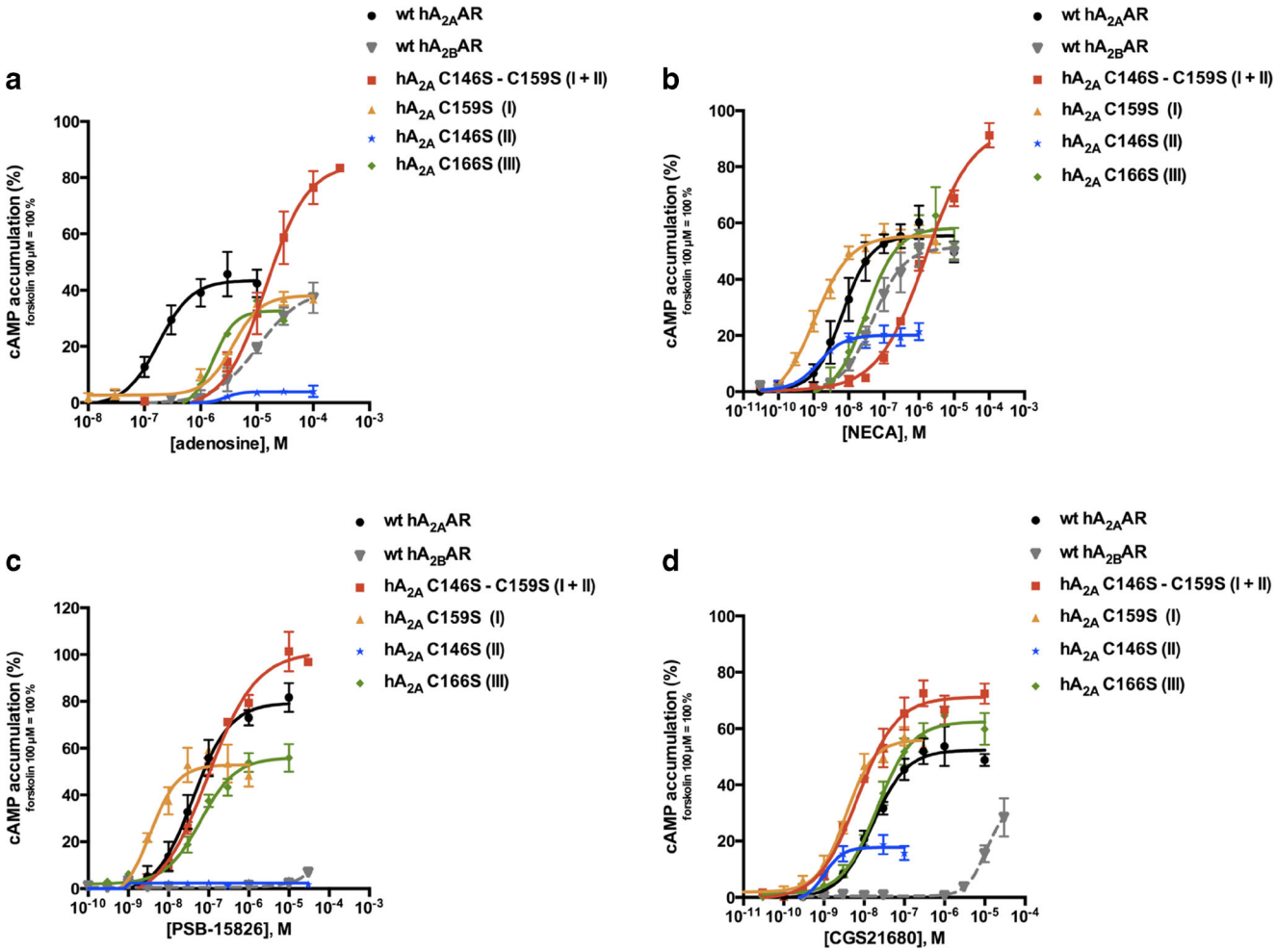

Fig. 4 Agonist-induced cAMP accumulation studies in CHO cells stably expressing the wt human A_{2A}AR, the wt human A_{2B}AR, or the A_{2A} cysteine mutant receptors. Cells were stimulated with different concentrations of selected agonists: adenosine (**a**), NECA (**b**), PSB-15826 (**c**), and CGS21680 (**d**). Data are normalized to forskolin (100 μM), set as 100 %. The disrupted disulfide bond is indicated in *brackets*. Data represent mean ± SEM of at least three independent experiments performed in duplicates. EC_{50} values and maximal effects are listed in Table 2

[^{3}H]NECA was used for the A_{2A} C146S mutant receptor because of the narrow window between total binding and non-specific binding values obtained with the radioligand [^{3}H]CGS21680. A significant loss in affinity was noticed for NECA itself in comparison to the wt A_{2A}AR (K_i values: 7.06 ± 1.27 vs. 39.1 ± 1.3 nM, see Table 3).

Binding mode and interactions

To understand the significance of extracellular disulfide bonds for receptor function, and to find possible explanations for the results obtained in mutagenesis experiments, we explored the X-ray crystal structures available for the A_{2A}AR co-crystallized with some of the ligands used in this study. A recent co-crystal structure with the agonist CGS21680 (4UHR.pdb) was considered as a reference, and two other structures crystallized with the agonists NECA (2YDV.pdb) and adenosine (2YDO.pdb) were superimposed. For the adenosine derivative PSB-15826, a putative binding mode was predicted by docking of the compound into the known orthosteric binding site of the A_{2A}AR. The docking calculation was evaluated by redocking of the co-crystallized agonist CGS21680 which yielded a root-mean-square deviation (RMSD) value of 0.90 Å. The results for PSB-15826 showed that the lowest binding energy binding pose was well correlated with the binding conformation of CGS21680. Similar to the binding interactions of adenosine (Fig. 6), NECA (Supplementary Fig. 1a), and CGS21680 (Supplementary Fig 1b), the adenine moiety of PSB-15826 forms a π-π interaction with Phe168, a hydrophobic interaction with Leu249 and hydrogen bond interactions with the amino acids residue Asn253 and Glu169 (Supplementary Fig 1c and 2). The 2′-OH function of the ribose interacts with Ser277, and the 3′-OH group possibly forms interactions with His278

Table 2 EC_{50} values and efficacies of selected A_{2A} agonists determined in cAMP accumulation assays at the wt $hA_{2A}AR$, the wt $hA_{2B}AR$, and the A_{2A} cysteine mutant receptors. Data are normalized to 100 μM forskolin, set as 100 %, and represent mean ± SEM of the three independent experiments, unless otherwise noted

Compounds		hA_{2A} wt	hA_{2B} wt	hA_{2A} C146S	hA_{2A} C166S	hA_{2A} C159S	hA_{2A} C146S – C159S
Adenosine	EC_{50} ± SEM (nM)	170 ± 29	11,900 ± 670***	n.d.	5110 ± 32$^{a, ***}$	3670 ± 719**	43,100 ± 8090$^{a, **}$
	Efficacy ± SEM (%)	44 ± 3	40 ± 6^{ns}	4 ± 1**	33 ± 2^{ns}	38 ± 2^{ns}	85 ± 8**
NECA	EC_{50} ± SEM (nM)	10.5 ± 0.8	109 ± 37**	1.43 ± 0.43***	31.4 ± 7.4$^{a, ns}$	1.27 ± 0.24***	870 ± 107**
	Efficacy ± SEM (%)	55 ± 3	51 ± 4^{ns}	20 ± 1**	58 ± 3^{ns}	55 ± 2^{ns}	94 ± 4**
CGS21680	EC_{50} ± SEM (nM)	16.6 ± 0.1	31,100 ± 7130***	0.653 ± 0.055***	25.9 ± 1.1$^{a, **}$	3.05 ± 0.15***	7.16 ± 1.59**
	Efficacy ± SEM (%)	52 ± 2	33 ± 7^{ns}	18 ± 1*	62 ± 2^{ns}	56 ± 2^{ns}	71 ± 2*
PSB-15826	EC_{50} ± SEM (nM)	62.0 ± 14.8	n.d.	n.d.	75.0 ± 16.6^{ns}	2.41 ± 0.79*	83.5 ± 4.1^{ns}
	Efficacy ± SEM (%)	79 ± 4	No increase	No increase	56 ± 3**	53 ± 3**	101 ± 4*

$^{n.d.}$ not determined; ^{ns} not significantly different from wt $hA_{2A}AR$ (determined using the two-tailed *t* test)

^{a} $n = 4$

* $p < 0.05$

** $p < 0.01$

*** $p < 0.001$

(Supplementary Fig 1c). The *N*-ethylcarboxamido group of NECA and CGS21680 was replaced with a hydroxymethylene group in PSB-15826 which forms interactions with Thr88 (Supplementary Fig 1c and 2d). In comparison, the *N*-ethylcarboxamido group binds to Thr88 and His250 (Supplementary Fig 1b). The 2-(4-(4-fluorophenyl)piperazin-1-yl)ethylthio group of PSB-15826 might form hydrophobic interactions with the residues Ile66 and Leu167 similar to the (2-carboxyethyl)phenylethylamino group of CGS21680. On the other hand, the negatively charged carboxy function of CGS21680 and the fluorophenyl group of PSB-15826, which acquires a partial negative charge, might be similarly hydrated in the extracellular space (Supplementary Fig 2 c–d). This network stabilizes the receptor-ligand complex beyond the interactions with the core adenosine structure located in the orthosteric binding site of the receptor.

Models of cysteine mutant adenosine A_{2A} receptors

A model of each of the cysteine mutant A_{2A} receptors was generated using the crystallographic structure of the human $A_{2A}AR$ bound to CGS21680 (4UHR.pdb) as a reference. Disulfide bond I ($Cys71^{2.69}$-$Cys159^{45.43}$) is formed in the middle of ECL2, and its disruption would increase the flexibility of the entire loop, in particular of two amino acids close to Cys159, Gln157, and Gln163, which might then form interactions with distant residues (Fig. 7a). When disulfide bond II ($Cys74^{3.22}$-$Cys146^{45.30}$) is disrupted (Fig. 7b) by the C146S mutation, Ser146 is found in close proximity to polar residues such as His75 and Asn144, with which it might form interactions. In the wt $A_{2A}AR$, the $Cys166^{45.50}$ residue is found in proximity to two residues involved in ligand binding, Phe168 and Glu169. The C166S mutation causing the disruption of disulfide bond III ($Cys77^{3.25}$-$Cys166^{45.50}$) may cause a rearrangement of those amino acids (Fig. 7c). Finally, the double mutant $A_{2A}AR$, in which disulfide bonds I and II are disrupted, is characterized by a high flexibility of ECL1 and 2 (Fig. 7d) influencing the orthosteric binding pocket as well. Several charged amino acids close to the mutated $Cys146^{45.30}$and $Cys159^{45.43}$, especially Lys150 and Lys153, become more flexible and free to form new interactions.

Discussion

The similarity in the orthosteric binding pockets of the four AR subtypes impedes the discovery of receptor subtype-selective drugs [44]. Structural investigation of adenosine receptors (ARs) is therefore critical for rational drug discovery.

A landmark in the analysis of the structure of ARs was the first X-ray structure of the $A_{2A}AR$ published in 2008 bound to the antagonist ZM241385 [25]. Subsequently, several other A_{2A} co-crystal structures were solved with a wide range of ligands, including NECA, adenosine [31], XAC, caffeine [45], UK-432097 [46], and CGS21680 [32]. The $A_{2A}AR$ was captured in different conformational states, inactive states [25, 30, 45, 47], intermediate states [31], and fully activated conformations [32, 46]. Due to their high flexibility and conformational diversity, the extracellular loops (ECLs) of the $A_{2A}AR$ have been resolved only in a few of the available crystal structures but the presence of disulfide bonds between ECLs has been consistently demonstrated in each of these X-ray structures [30–32]. Three disulfide bonds constrain ECL1 and ECL2, $Cys71^{2.69}$-$Cys159^{45.43}$ (I), $Cys74^{3.22}$-$Cys146^{45.30}$

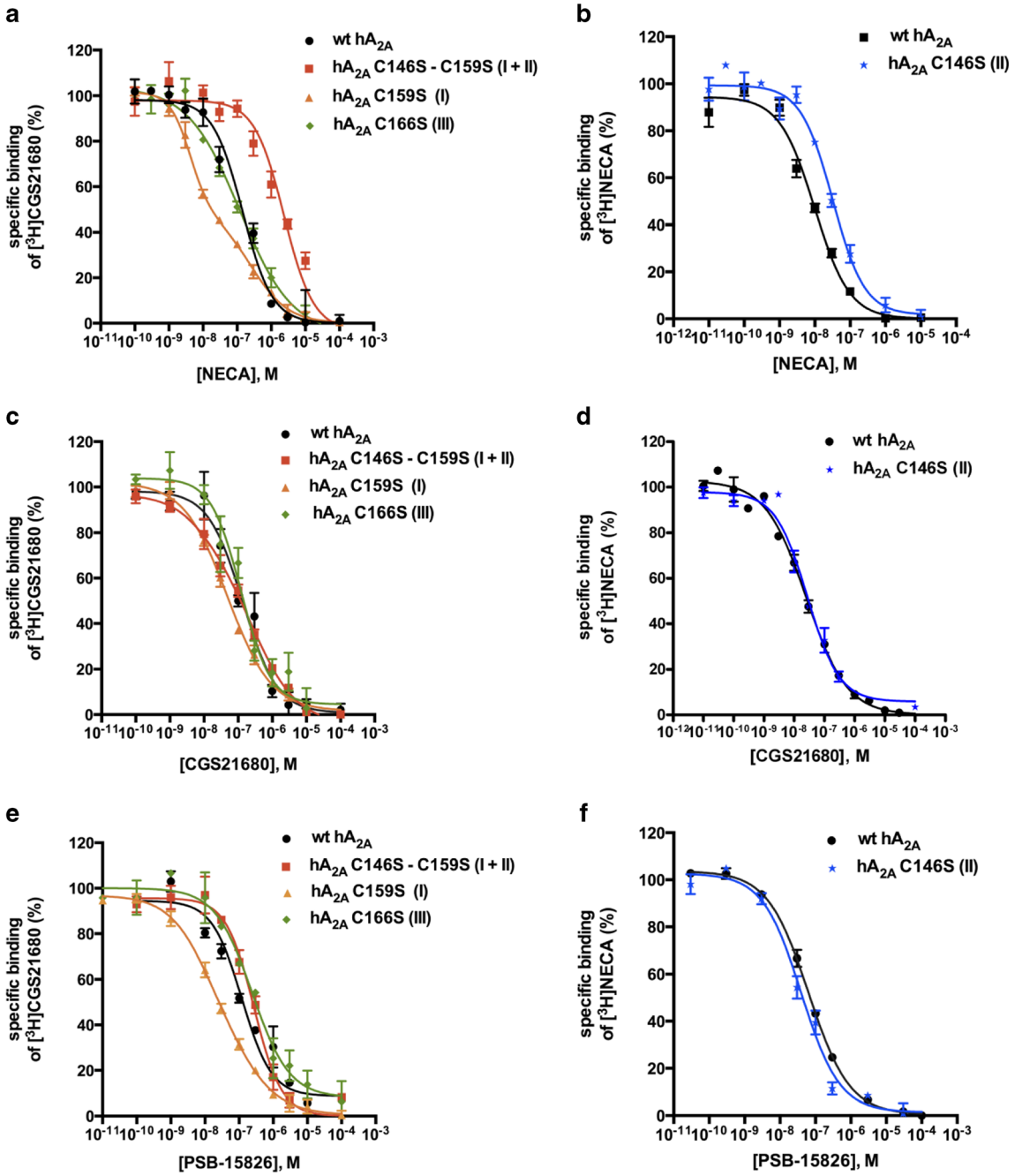

Fig. 5 Competition binding studies at the wild type (wt) human A_{2A}AR and the A_{2A} cysteine mutants versus [^{3}H]CGS21680 (5 nM; **a**, **c**, **e**) or [^{3}H]NECA (3 nM; **b**, **d**, **f**). The agonists NECA (**a**, **b**), CGS21680 (**c**, **d**), and PSB-15826 (**e**, **f**) were tested. The affinity of the agonists at the hA_{2A} C146S mutant receptor could only be defined with [^{3}H]NECA as radioligand due to the low mutant expression level and the higher affinity of [^{3}H]NECA as compared to [^{3}H]CGS21680. The disrupted disulfide bond number is indicated in *brackets*. Data points represent means ± SEM of at least three independent experiments performed in duplicates. K_i values are listed in Table 3

(II), and Cys77$^{3.25}$-Cys166$^{45.50}$ (III), see Fig. 2. The latter is conserved among most of the rhodopsin-like class A GPCRs [28]. A fourth intra-loop disulfide bond is present in the ECL3 (Cys259$^{6.61}$-Cys262$^{6.64}$).

The two closely related A_{2A} and A_{2B}AR subtypes are characterized by a high sequence identity (58 %). Nevertheless, the endogenous ligand adenosine (**1**) and most of its derivatives display much higher affinity for the A_{2A}AR as compared to the A_{2B}AR (70-fold difference in EC_{50} values in our experiments: 170 vs. 11900 nM, see Table 2). Contradictory data were also found regarding the essential cysteine residues and extracellular disulfide bonds present in the two AR subtypes. While crystal structures and a recent molecular modeling study indicated that the four extracellular

Table 3 Affinities of selected ligands for the wt human A_{2A}AR compared to the cysteine mutant receptors determined in radioligand binding studies versus [^{3}H]CGS21680 (5 nM) or [^{3}H]NECA (3 nM). K_i values were calculated based on the K_D values obtained in homologous competition experiments (see Table 1). Data are mean ± SEM of the three independent experiments, otherwise noted

K_i ± SEM (nM)						
[^{3}H]CGS21680	NECA	Fold shift[d]	CGS21680	Fold shift[d]	PSB-15826	Fold shift[d]
hA_{2A} wt	81.2 ± 11.4[a]		130 ± 1[a]		118 ± 1	
hA_{2A} C166S	99.4 ± 15.2[ns]	1.2	114 ± 4[b, ns]	0.9	196 ± 1[***]	1.7
hA_{2A} C159S	Low[c] 4.92 ± 0.68[*] High 467 ± 119[*]	0.1 5.8	50.1 ± 0.7[b, ***]	0.4	29.2 ± 3.6[a, ***]	0.3
	One-site 20.2 ± 0.8	0.3				
hA_{2A} C146S – C159S	2490 ± 3[b, ***]	31	128 ± 10[a, ns]	1.0	278 ± 8[a, ***]	2.4
[^{3}H]NECA						
hA_{2A} wt	7.06 ± 1.27		17.8 ± 3.5		43.5 ± 5.3	
hA_{2A} C146S	39.1 ± 1.3[***]	5.5	19.5 ± 3.4[ns]	1.1	33.9 ± 2.2[ns]	0.8

[a] $n = 4$

[b] $n = 5$

[c] Low and high refer to the two K_i values of the biphasic curve of the C159S mutant, while one-site refer to the single K_i value calculated with one-site competition fit

[d] The shift represents the ratio K_i (mutant):K_i (wt)

[ns] not significantly different from wt hA_{2A}AR (determined using the two-tailed t test)

[*] $p < 0.05$

[***] $p < 0.001$

disulfide bonds are formed in A_{2A}AR [25, 30–33], no crystal structure of the A_{2B}AR has been determined so far. Mutagenesis studies of extracellular cysteine residues of the A_{2B}AR subtype [11] demonstrated that for the A_{2B} subtype, only the two "GPCR-conserved" cysteine residues (Cys78$^{3.25}$-Cys171$^{45.50}$) located at the extracellular end of transmembrane domain 3 (TMD3) and in the ECL2 form a disulfide bond that is essential for ligand binding and receptor activation [11].

Several hypotheses might explain those discrepancies, e.g., the disulfide bonds observed in the A_{2A}AR crystal structures might be artifacts due to artificial conditions

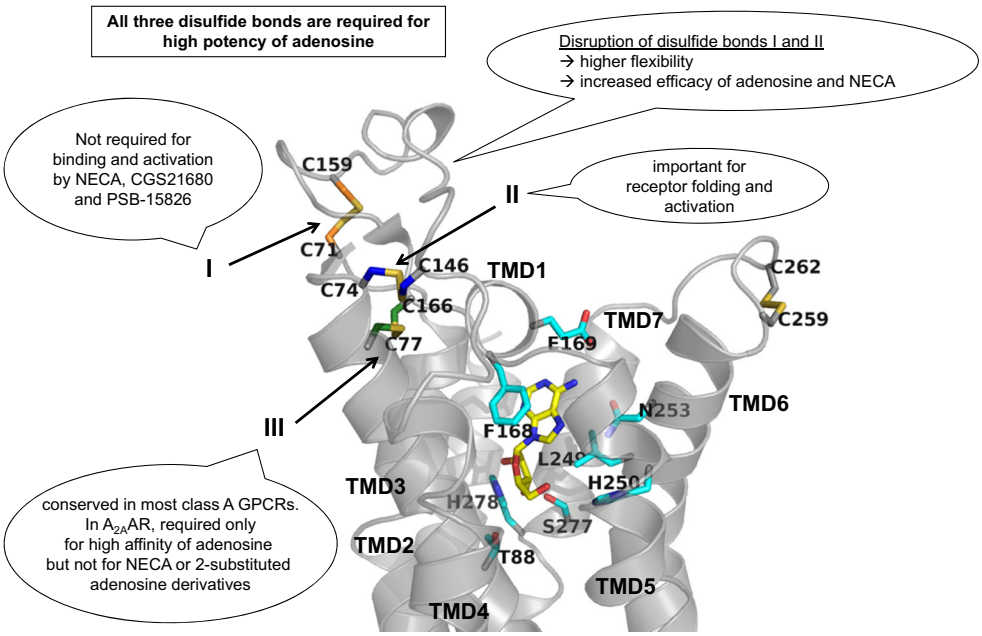

Fig. 6 Binding modes of adenosine in the A_{2A}AR. Crystallographic binding poses of the endogenous agonist adenosine (represented in *stick*, carbon atoms in *yellow*) in the binding pocket of the A_{2A}AR (represented as *gray ribbon*) are shown. The side chains of important residues in the binding pocket are shown as *sticks* with carbon atoms in *cyan*. The cysteine residues involved in disulfide bonds are shown as *sticks*, and the carbon atoms are color-coded (Cys71$^{2.69}$-Cys159$^{45.43}$ *orange*, Cys74$^{3.22}$-Cys146$^{45.30}$ *blue*, and Cys77$^{3.25}$-Cys166$^{45.50}$ *green*). The disulfide bond number is indicated. The main results are summarized in figure

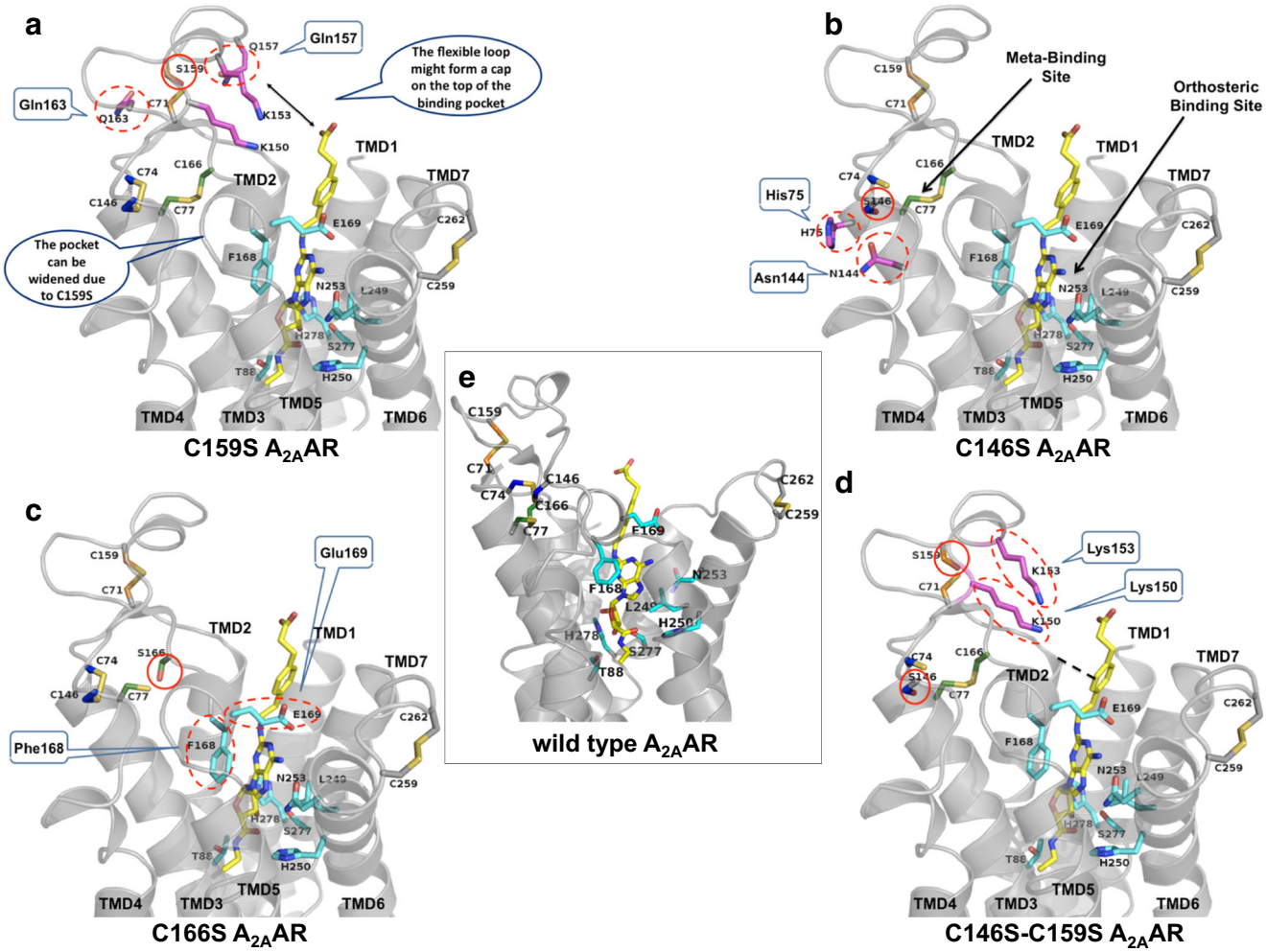

Fig. 7 3D homology models of A_{2A}AR wt and mutant receptors. The models of the four mutant and the wild type A_{2A} receptors are shown with the ligand CGS21680 (*stick* representation with carbons in *yellow*). The sidechains of important residues in the orthosteric binding pocket are shown as *sticks* with carbons in *cyan*. The cysteine residues involved in disulfide bonds are shown as *sticks*, and the carbon atoms are color-coded as before ($Cys71^{2.69}$-$Cys159^{45.43}$ *orange*, $Cys74^{3.22}$-$Cys146^{45.30}$ *blue*, and $Cys77^{3.25}$-$Cys166^{45.50}$ *green*). The mutated serine residues are shown in the respective color code as well. Amino acids which play an important role in the mutated receptors are highlighted as *sticks* with carbons in *magenta*, and predicted interactions are *encircled with dotted lines*. **a** Disruption of disulfide bond I ($Cys71^{2.69}$-$Cys159^{45.43}$ -> Ser159). **b** Disruption of disulfide bond II ($Cys74^{3.22}$-$Cys146^{45.30}$ -> Ser146). **c** Disruption of disulfide bond III ($Cys77^{3.25}$-$Cys166^{45.50}$ -> Ser166). **d** Disruption of disulfide bonds I and II (Ser159, Ser146). **e** Wild type A_{2A}AR model based on the CGS21680-bound crystal structure

during the crystallization process. Another explanation could be that the cysteine residues found to be not essential for the function of the A_{2B}AR might possess a different role, other than the formation of intramolecular disulfide bonds. In order to find out whether the predicted disulfide bonds in the A_{2A}AR are actually required for ligand binding and receptor function, a focused investigation was required.

The importance of A_{2A}AR disulfide bonds for [^{3}H]CGS21680 binding had previously been shown by pre-incubation with reducing agents, such as tris-(2-carboxyethyl)phosphine (TCEP) or dithiothreitol (DTT) [48, 49]. A recent mutagenesis approach suggested that the "GPCR-conserved" disulfide bond in the A_{2A}AR ($Cys77^{3.25}$-$Cys166^{45.50}$) was neither essential for its expression in the plasma membrane nor for high-affinity binding of [^{3}H]CGS21680 [35] indicating that this disulfide bond observed in the A_{2A}AR crystal structure might be an artifact. However, the published mutagenesis study [35] focused on radioligand binding experiments utilizing only a single adenosine derivative, CGS21680, while functional data were not measured. Our investigation included both, binding and functional analysis of several A_{2A}AR cysteine mutants, characterizing them with structurally diverse agonists. In addition, 3D homology models of the cysteine mutant receptors were generated. It should be emphasized that the models of the mutant receptors are speculative; nevertheless, they are useful and supported by our experimental data.

Extracellular disulfide bonds are important for high agonist potencies

Initially, we confirmed the relevance of disulfide bonds for the function of the A_{2A}AR: DTT pre-incubation, which leads to a disruption of accessible disulfide bonds by reducing them to thiols, led to a marked reduction in potency for agonists. The receptors could still be fully activated, but the curves were shifted to the right (Fig. 3). The effect was much more pronounced for the small nucleoside NECA (100-fold decrease in potency) than that for CGS21680 (5-fold decrease), which contains a large substituent in the 2-position that extends to the extracellular space. Thus, CGS21680 can rescue a large part of the potency lost by disulfide bond disruption probably by keeping the ECLs in a favorable conformation. DTT treatment will cause the disruption of all accessible disulfide bonds present in the A_{2A}AR; therefore, a precise understanding of the importance of single disulfide bonds for the stability and function of the receptor has not been feasible by that method.

Role of single extracellular disulfide bonds the in A_{2A}AR

In order to get a detailed view on the role of extracellular disulfide bonds of the A_{2A}AR, we generated mutant A_{2A} receptors in which cysteine residues were exchanged with serine (C146S, C159S, C166S, and a double mutant C146S-C159S) focusing on ligand binding and receptor function with various ligands (Fig. 1). We tested A_{2A}AR agonists with different substituents evaluating their effects on the mutant receptors, including the endogenous ligand adenosine (**1**); its ribose-modified derivative NECA (**2**); the A_{2A}-selective CGS21680 (**3**); a NECA derivative with a long, acidic substituent in the 2-position of the adenine core structure; and PSB-15826 (**4**), an adenosine derivative with a bulky 2-substituent that is also selective for the A_{2A}AR. After the CHO cell lines stably expressing the mutant receptors had been established, two approaches were used to determine AR expression levels: (i) by ELISA, we characterized the amount of ARs transported to the cell surface, and (ii) by radioligand binding on cell membranes, we determined A_{2A}AR expression in the membrane preparations (B_{max} value), see Table 1. All mutant receptors were expressed in the cell membrane with moderate differences in expression levels between 23–227 % of that of the wt A_{2A}AR (=100 %). Differences in B_{max} values determined in radioligand binding studies were smaller and dependent on the employed radioligand. By this method, using membrane preparations rather than whole cells, receptors expressed on intracellular cell organelles will be captured in addition to those in the outer cell membrane. All in all expression could be confirmed although the data obtained with various methods showed some differences.

The three extracellular disulfide bonds are critical for A_{2A}AR activation by adenosine

Each of the investigated cysteine mutations led to dramatic reductions in the potency of adenosine (Table 2; Supplementary Table 2). Disruption of disulfide bond I (C159S mutant) and III (C166S mutant) resulted in receptors at which adenosine had very low potency but was still able to fully activate the receptor. Thus, both mutant receptors behaved similarly as the wt A_{2B}AR, which is a "low-affinity" AR subtype, towards adenosine, see Fig. 4 [50]. Disruption of disulfide bond II in the C146S mutant yielded a receptor that could hardly be activated anymore by adenosine, while the disruption of both disulfide bonds I and II was activatable by adenosine, but with very low potency. Thus, all the three disulfide bonds appeared to be critical for the response of the A_{2A}AR induced by the endogenous agonist adenosine (Table 2; Supplementary Table 2). Surprisingly, this was not the case for other agonists, even those with close structural similarity such as NECA (see below). All observed effects were strongly dependent on the agonist's structure under study (Supplementary Table 2). Thus, it appears to be essential to always investigate effects using the relevant ligand, and not a surrogate compound.

Disruption of disulfide bond I

The C159S mutant receptor, in which the first, most extracellular disulfide bond is disrupted, could be fully activated by all the four investigated agonists, see Fig. 4. While adenosine showed significantly reduced potency, the affinities and potencies of the other agonists, NECA, CGS21680, and PSB-15826, were increased (Tables 2 and 3; Supplementary Table 1). This effect might partly be due to the 2-fold higher expression level of this mutant in comparison to the wt A_{2A}AR as determined by ELISA (Table 1). The disulfide bond I ($Cys71^{2.69}$-$Cys159^{45.43}$) restricts the movement of the receptor, and the amino acid residues Gln157 or Gln163, which are close to Cys159, form an interaction network in proximity to the natural ligand adenosine (Figs. 6 and 7a). This could explain the significant loss in potency for adenosine when $Cys159^{45.43}$ was mutated (Table 2) and the interaction network was disrupted. In the C159S mutant receptor, the orthosteric ligand binding pocket will become wider than in the wild type receptor (Fig. 7a), which could then lead to a reduced affinity for adenosine.

Besides the orthosteric binding site, a so-called meta-binding site has been postulated by Moro et al. [51], which is thought to be responsible for initial ligand-receptor contacts and may serve as a pre-filter. Moro et al. investigated the A_{2A}AR using a molecular dynamics simulation approach, termed "supervised molecular dynamics" (SuMD). Using various adenosine receptor ligands, they detected for adenosine

and NECA a meta-binding site in the loop region, to which the affinity of the ligands appeared to be almost as strong as for the orthosteric binding site. In our receptor, mutant adenosine might stay longer in the meta-binding site as compared to the orthosteric binding site due to stronger interactions (Fig. 7a). The presence of a high-affinity meta-binding site might also be an explanation for the biphasic binding curve observed for NECA (Fig. 5a). Another explanation could be the presence of mono- and di- or multimeric receptor species with different affinities for NECA.

Contrarily, the agonists NECA (containing a carboxamido-modified ribose), and the much larger 2-substituted nucleosides CGS21680 (NECA derivative) and PSB-15826 (adenosine derivative) can probably form more interactions than adenosine itself with the mutated receptor resulting in higher affinity for the orthosteric binding site (Table 3; Figs. 5 and 7a). Residues in the loop region such as Lys150 or Lys153 are predicted to form interactions with the large agonists CGS21680 and PSB-15826 thereby increasing affinity and potency of the ligands at the more flexible mutant receptor (Fig. 7a).

Disruption of disulfide bond II

The mutation of Cys146$^{45.30}$ leading to the disruption of disulfide bond II in the A_{2A}AR led to an about 4-fold reduced cell surface expression of the receptor as determined by ELISA (Table 1). Similar results had been reported by Naranjo et al. for the corresponding C146A mutant, in which cysteine 146 was replaced by alanine instead of serine [35]. These data suggest that the disulfide bond Cys74$^{3.22}$-Cys146$^{45.30}$ connecting TMD3 and ECL2 is important for correct folding of the receptor, and its disruption might cause receptor aggregation and retention in the endoplasmatic reticulum, as it was previously proposed for other cysteine mutant GPCRs [20, 52]. The C146S mutant receptors that were transported to the plasma membrane may have adopted a different, stabilized conformation due to new interactions which are formed with the exchanged serine residue. The side chain of serine is sterically and electronically similar to cysteine and could form a hydrogen bond with the nearby residue Asn144 or with His75 (Fig. 7b).

Both, adenosine and its 2-substituted derivative PSB-15826, were virtually unable to activate the mutant receptor (Fig. 4; Table 2), while the other investigated agonists (NECA and the NECA derivative CGS21680) showed significantly reduced efficacies as compared to the wt A_{2A}AR (Fig. 4; Table 2). However, affinities and potencies of NECA and CGS21680 did not seem to be much affected (Supplementary Table 1 and 2). Interestingly, the adenosine derivative PSB-15826 displayed unaltered, high binding affinity for the mutant A_{2A}AR, despite its inability to activate the receptor (Tables 2 and 3).

The mutation of Cys146$^{45.30}$ may lead to the stabilization of an inactive conformational state of the A_{2A}AR, which abolishes (in case of adenosine derivatives) or hampers (in case of NECA derivatives) receptor activation (Fig. 7b). The *N*-ethylcarboxamido group of NECA and CGS21680 may act as an anchor that facilitates the induction of a conformational change of the receptor eventually leading to G protein activation. In the related A_{2B}AR subtype, disulfide bond II is not present due to the lacking of corresponding cysteine residues (Supplementary Table 1).

Disruption of the "GPCR-conserved" disulfide bond III

C166S mutation led to the disruption of disulfide bond III (Cys77$^{3.25}$-Cys166$^{45.50}$) in the A_{2A}AR, which is typically conserved in most rhodopsin-like GPCRs. The loss of this disulfide bond led to a strong reduction in potency for adenosine (30-fold), but not for the other investigated agonists (Table 2 and Supplementary Table 2). All of them showed similarly high potency and affinity at the mutant as compared to the wt receptor (Tables 2 and 3; Supplementary Table 2). Efficacy of all agonists including adenosine was also quite similar or only slightly lower (in case of PSB-15826) as for the wt A_{2A}AR (Fig. 4; Table 2).

As shown in Fig. 7c, the location of two of the residues important for the interaction with the adenine core of nucleosidic agonists, Phe168 and Glu169, might be affected by the loss of the disulfide bond when Cys166$^{45.50}$ is mutated, since it is very close to the disulfide bond. Thus, the conserved disulfide bond Cys77$^{3.25}$-Cys166$^{45.50}$ (III) appears to be essential for high affinity of the endogenous ligand adenosine.

The adenosine derivatives NECA, CGS21680, and PSB-15826 are characterized by modifications and substitutions of the ribose moiety, or the adenine core, respectively, which interact with the A_{2A}AR receptor, and appear to be thereby able to compensate for the effect of the "GPCR-conserved" disulfide bond disruption (Supplementary Table 2). Comparison of adenosine (30-fold loss in potency) and NECA (minor loss) confirms that the *N*-ethylcarboxamido group largely contributes to the stabilization of the ligand-receptor complex (Table 2 and Supplementary Table 2). This finding is supported by the results obtained for the NECA derivative CGS21680 which is equally potent at the mutant and the wt A_{2A}AR (Fig. 4; Table 2). Despite the fact that PSB-15826 has no NECA modification on the ribose ring, its potency at the mutant receptor is comparable to that at the wt A_{2A}AR (Table 2) because the long 2-substituent which extends to the extracellular space stabilizes the receptor and compensates for the disrupted disulfide bond by forming other interaction networks (Fig. 7c).

Concurrent disruption of disulfide bonds I and II

In the double mutant receptor C146S-C159S, the two "non-GPCR-conserved" disulfide bonds I and II (Cys71$^{2.69}$-Cys159$^{5.20}$ and Cys74$^{3.22}$-Cys146$^{4.67}$), close to the extracellular surface, were disrupted.

Functional studies showed that the potency and efficacy at this mutant receptor are affected by the length of the substitution in position 2 at the adenine moiety of the ligand (Tables 2 and 3; Supplementary Table 1). Small ligands such as adenosine and NECA showed a considerable loss in potency and affinity in the double mutant receptor (253-fold decreased potency for adenosine, 87-fold loss in potency/31-fold decrease in affinity for NECA) as compared to the wt A_{2A}AR, see Tables 2 and 3. On the other hand, 2-substituted adenosine derivatives like CGS21680 and PSB-15826 only showed minor changes in potency and affinity in comparison to the wt A_{2A}AR (Table 3).

The disruption of the two most extracellular disulfide bonds in the double mutant receptor probably results in high flexibility of ECL1 and ECL2 (Fig. 7d). The double disruption could also influence TMD2 and TMD3 of the receptor and furthermore, affect the conformation of amino acid residues located in the orthosteric binding pocket. The high flexibility of the loops will therefore affect the interaction of the A_{2A}AR with the agonists in the binding site, as observed for the small ligands adenosine and NECA (Supplementary Table 1 and 2). However, in case of the agonists that feature an extended 2-substituent, the flexible ECL2 of the double mutant receptor may be stabilized by that large substituent of CGS21680 and PSB-15826, resulting in similar potency and efficacy as at the wt A_{2A}AR (Supplementary Table 2). Probably, as already explained for the C159S mutant, the charged amino acid residues Lys150 or Lys153 are likely to form interactions with CGS21680 and PSB-15826 and contribute to the fact that these agonists show similar potency and affinity at the double mutant as at the wt A_{2A}AR (Fig. 7d).

The smaller agonists adenosine and NECA displayed higher efficacy at the double mutant receptor as compared to the wt A_{2A}AR (85 and 94 % vs. 44 and 55 % for the wt A_{2A}AR, respectively; see Table 2). Those small ligands are not expected to stabilize the flexible ECL2 of the double mutant receptor. Due to the lacking of the two disulfide bonds, the mutant receptor will be more flexible, and the equilibrium between receptor conformations may be more easily shifted towards an active conformation.

Conclusions

Functional studies indicated that all the three disulfide bonds between ECL1 and 2 of the A_{2A}AR are essential for high potency of the receptor for the endogenous agonist adenosine (Fig. 4 and Table 2). At present, it cannot be excluded that the formation of the extracellular disulfide bonds of the cysteine-rich A_{2A}AR is dynamic as suggested for other GPCRs including the closely related A_{2B}AR [11] and the $P2Y_{12}$ receptor [17, 50]. The dynamic and emergent disruption of extracellular disulfide bonds may add another level of GPCR modulation in general, and of the regulation of A_{2A} and A_{2B}AR function in particular.

Acknowledgments E.D.F., A.C.S., and C.E.M. were supported by the German Federal Ministry of Education and Research (BMBF project Bonn International Graduate School in Drug Sciences (BIGS DrugS)) and by the State of North-Rhine Westfalia (NRW International Research Graduate School BIOTECH-PHARMA).

Compliance with ethical standards

Conflict of interest The authors declare that they have no conflict of interest.

References

1. Fredholm BB, IJzerman AP, Jacobson KA, Linden J, Müller CE (2011) International union of basic and clinical pharmacology. LXXXI. Nomenclature and classification of adenosine receptors—an update. Pharmacol Rev 63:1–34
2. Jacobson KA, Müller CE (2015) Medicinal chemistry of adenosine, P2Y and P2X receptors. Neuropharmacology. doi:10.1016/j.neuropharm.2015.12.001
3. Fredholm BB (2007) Adenosine, an endogenous distress signal, modulates tissue damage and repair. Cell Death Differ 14:1315–23
4. Hasko G, Linden J, Cronstein B, Pacher P (2008) Adenosine receptors: therapeutic aspects for inflammatory and immune diseases. Nat Rev Drug Discov 7:759–70
5. Boros D, Thompson J, Larson D (2015) Adenosine regulation of the immune response initiated by ischemia reperfusion injury. Perfusion. doi:10.1177/0267659115586579
6. Eltzschig HK, Carmeliet P (2011) Hypoxia and inflammation. N Engl J Med 364:656–65
7. Eltzschig HK, Sitkovsky M, Robson SC (2012) Purinergic signaling during inflammation. N Engl J Med 367:2322–33
8. Antonioli L, Blandizzi C, Pacher P, Haskó G (2013) Immunity, inflammation and cancer: a leading role for adenosine. Nat Rev Cancer 13:842–57
9. Leone RD, Lo Y-C, Powell JD (2015) A_{2A}AR antagonists: next generation checkpoint blockade for cancer immunotherapy. Comput Struct Biotechnol J 13:265–72
10. Müller CE, Jacobson KA (1808) Recent developments in adenosine receptor ligands and their potential as novel drugs. Biochim Biophys Acta 2011:1290–308
11. Schiedel AC, Hinz S, Thimm D, Sherbiny F, Borrmann T, Maass A et al (2011) The four cysteine residues in the second extracellular loop of the human adenosine A_{2B} receptor: role in ligand binding and receptor function. Biochem Pharmacol 82:389–99
12. Jaakola V-P, Lane JR, Lin JY, Katritch V, Ijzerman AP, Stevens RC (2010) Ligand binding and subtype selectivity of the human A_{2A} adenosine receptor: identification and characterization of essential amino acid residues. J Biol Chem 285:13032–44

13. El Maatougui A, Azuaje J, Gonzàalez-Gòmez M, Miguez G, Crespo A, Carbajales C et al (2016) Discovery of potent and highly selective A_{2B} adenosine receptor antagonist chemotypes. J Med Chem. doi:10.1021/acs.jmedchem.5b01586
14. Peeters MC, van Westen GJP, Li Q, IJzerman AP (2011) Importance of the extracellular loops in G protein-coupled receptors for ligand recognition and receptor activation. Trends Pharmacol Sci 32:35–42
15. Ni F, So S-P, Cervantes V, Ruan K-H (2008) A profile of the residues in the second extracellular loop that are critical for ligand recognition of human prostacyclin receptor. FEBS J 275:128–37
16. Ott TR, Troskie BE, Roeske RW, Illing N, Flanagan CA, Millar RP (2002) Two mutations in extracellular loop 2 of the human GnRH receptor convert an antagonist to an agonist. Mol Endocrinol 16: 1079–88
17. Ahn KH, Bertalovitz AC, Mierke DF, Kendall DA (2009) Dual role of the second extracellular loop of the cannabinoid receptor 1: ligand binding and receptor localization. Mol Pharmacol 76:833–42
18. Olah ME, Jacobson KA, Stiles GL (1994) Role of the second extracellular loop of adenosine receptors in agonist and antagonist binding. Analysis of chimeric A_1/A_3 adenosine receptors. J Biol Chem 269:24692–8
19. Seibt BF, Schiedel AC, Thimm D, Hinz S, Sherbiny FF, Müller CE (2013) The second extracellular loop of GPCRs determines subtype selectivity and controls efficacy as evidenced by loop exchange study at A_2 adenosine receptors. Biochem Pharmacol 85:1317–29
20. Zhang K, Zhang J, Gao Z-G, Zhang D, Zhu L, Han GW et al (2014) Structure of the human $P2Y_{12}$ receptor in complex with an antithrombotic drug. Nature 509:115–8
21. Avlani VA, Gregory KJ, Morton CJ, Parker MW, Sexton PM, Christopoulos A (2007) Critical role for the second extracellular loop in the binding of both orthosteric and allosteric G protein-coupled receptor ligands. J Biol Chem 282:25677–86
22. Unal H, Jagannathan R, Bhat MB, Karnik SS (2010) Ligand-specific conformation of extracellular loop 2 in the angiotensin II type 1 receptor. J Biol Chem 285:16341–50
23. Klco JM, Wiegand CB, Narzinski K, Baranski TJ (2005) Essential role for the second extracellular loop in C5a receptor activation. Nat Struct Mol Biol 12:320–6
24. De Graaf C, Foata N, Engkvist O, Rognan D (2008) Molecular modeling of the second extracellular loop of G protein-coupled receptors and its implication on structure-based virtual screening. Proteins 71:599–620
25. Jaakola V, Griffith MT, Hanson MA, Cherezov V, Ellen YT, Lane JR et al (2008) The 2.6 angstrom crystal structure of a human A_{2A} adenosine receptor bound to an antagonist. Science 322:1211–7
26. Sherbiny FF, Schiedel AC, Maass A, Müller CE (2009) Homology modelling of the human adenosine A2B receptor based on X-ray structures of bovine rhodopsin, the beta2-adrenergic receptor and the human adenosine A2A receptor. J Comput Aided Mol Des 23: 807–28
27. Rader AJ, Anderson G, Isin B, Khorana HG, Bahar I, Klein-Seetharaman J (2004) Identification of core amino acids stabilizing rhodopsin. Proc Natl Acad Sci U S A 101:7246–51
28. Katritch V, Cherezov V, Stevens RC (2013) Structure-function of the G protein-coupled receptor superfamily. Annu Rev Pharmacol Toxicol 53:531–56
29. Ballesteros JA, Weinstein H (1995) Integrated methods for the construction of three-dimensional models and computational probing of structure-function relations in G protein-coupled receptors. Methods Neurosci 25:366–428
30. Liu W, Chun E, Thompson AA, Chubukov P, Xu F, Katritch V et al (2012) Structural basis for allosteric regulation of GPCRs by sodium ions. Science 337:232–6
31. Lebon G, Warne T, Edwards PC, Bennett K, Christopher J, Leslie AGW et al (2011) Agonist-bound adenosine A_{2A} receptor structures reveal common features of GPCR activation. Nature 474:521–5
32. Lebon G, Edwards PC, Leslie AGW, Tate CG (2015) Molecular determinants of CGS21680 binding to the human adenosine A_{2A} receptor. Mol Pharmacol 87:907–15
33. Goddard WA, Kim S-K, Li Y, Trzaskowski B, Griffith AR, Abrol R (2010) Predicted 3D structures for adenosine receptors bound to ligands: comparison to the crystal structure. J Struct Biol 170:10–20
34. Zhang K, Zhang J, Gao Z-G, Zhang D, Zhu L, Han GW et al (2014) Agonist-bound structure of the human $P2Y_{12}$ receptor. Nature 509: 119–22
35. Naranjo AN, Chevalier A, Cousins GD, Ayettey E, McCusker EC, Wenk C et al (1848) Conserved disulfide bond is not essential for the adenosine A_{2A} receptor: extracellular cysteines influence receptor distribution within the cell and ligand-binding recognition. Biochim Biophys Acta 2015:603–14
36. Markowitz D, Goff S, Bank A (1988) A safe packaging line for gene transfer: separating viral genes on two different plasmids. J Virol 62:1120–4
37. Nordstedt C, Fredholm BB (1990) A modification of a protein-binding method for rapid quantification of cAMP in cell culture supernatants and body fluid. Anal Biochem 189: 231–4
38. Backliwal G, Hildinger M, Kuettel I, Delegrange F, Hacker DL, Wurm FM (2008) Valproic acid: a viable alternative to sodium butyrate for enhancing protein expression in mammalian cell cultures. Biotechnol Bioeng 101:182–9
39. Bradford M (1976) Rapid and sensitive method for quantification of microgram quantities of protein utilizing principle of protein-dye binding. Anal Biochem 72:248–54
40. Morris GM, Huey R, Lindstrom W, Sanner MF, Belew RK, Goodsell DS et al (2009) AutoDock4 and AutoDockTools4: automated docking with selective receptor flexibility. J Comput Chem 30:2785–91
41. Computing GC, Inc. Molecular Operating Environment (MOE) 2014.09 2014.
42. Hillmann P, Ko G, Spinrath A, Raulf A, Von Ku I, Wolff SC et al (2009) Key determinants of nucleotide-activated G protein-coupled $P2Y_2$ receptor function revealed by chemical and pharmacological experiments, mutagenesis and homology modeling. J Med Chem 52:2762–75
43. Murphree LJ, Marshall MA, Rieger JM, MacDonald TL, Linden J (2002) Human A_{2A} adenosine receptors: high-affinity agonist binding to receptor-G protein complexes containing Gβ4. Mol Pharmacol 61:455–62
44. Katritch V, Kufareva I, Abagyan R (2011) Structure based prediction of subtype selectivity for adenosine receptor antagonists. Neuropharmacology 60:108–15
45. Doré AS, Robertson N, Errey JC, Ng I, Hollenstein K, Tehan B et al (2011) Structure of the adenosine A_{2A} receptor in complex with ZM241385 and the xanthines XAC and caffeine. Structure 19: 1283–93
46. Xu F, Wu H, Katritch V, Han GW, Jacobson KA, Gao Z-G et al (2011) Structure of an agonist-bound human A_{2A} adenosine receptor. Science 332:322–7
47. Hino T, Arakawa T, Iwanari H, Yurugi-kobayashi T (2012) G protein-coupled receptor inactivation by an allosteric inverse agonist antibody. Nature 482:237–40
48. O'Malley MA, Naranjo AN, Lazarovab T, Robinson AS (2010) Analysis of adenosine A_{2A} receptor stability: effects of ligands and disulfide bonds. Biochemistry 49: 9181–9

49. Mazzoni MR, Giusti L, Rossi E, Taddei S, Lucacchini A (1997) Role of cysteine residues of rat A_{2A} adenosine receptors in agonist binding. Biochim Biophys Acta 1324:159–70
50. Müller CE, Scior T (1993) Adenosine receptors and their modulators. Pharm Acta Helv 68:77–111
51. Sabbadin D, Moro S (2014) Supervised molecular dynamics (SuMD) as a helpful tool to depict GPCR-ligand recognition pathway in a nanosecond time scale. J Chem Inf Model 54:372–6
52. Scholl DJ, Wells JN (2000) Serine and alanine mutagenesis of the nine native cysteine residues of the human A_1 adenosine receptor. Biochem Pharmacol 60:1647–54